Correlated Ion Transport and the Gel Phase in Room Temperature Ionic Liquids

Michael McEldrew,[†] Zachary A. H. Goodwin,[‡,¶] Hongbo Zhao,[†] Martin Z. Bazant,[*,†,§] and Alexei A. Kornyshev[*,‡,¶,‖]

[†]*Department of Chemical Engineering, Massachusetts Institute of Technology, Cambridge, MA, USA*

[‡]*Department of Chemistry, Imperial College of London, Molecular Sciences Research Hub, White City Campus, Wood Lane, London W12 0BZ, UK*

[¶]*Thomas Young Centre for Theory and Simulation of Materials, Imperial College of London, South Kensington Campus, London SW7 2AZ, UK*

[§]*Department of Mathematics, Massachusetts Institute of Technology, Cambridge, MA, USA*

[‖]*Institute of Molecular Science and Engineering, Imperial College of London, South Kensington Campus, London SW7 2AZ, UK*

E-mail: bazant@mit.edu; a.kornyshev@imperial.ac.uk

Abstract

Here we present a theory of ion aggregation and gelation of room temperature ionic liquids (RTILs). Based on it, we investigate the effect of ion aggregation on correlated ion transport - ionic conductivity and transference numbers - obtaining closed-form expressions for these quantities. The theory depends on the maximum number of associations a cation and anion can form, and the strength of their association. To validate the presented theory, we perform molecular dynamics simulations on several RTILs, and a range of temperatures for one RTIL. The simulations indicate the formation of

large clusters, even percolating through the system under certain circumstances, thus forming a gel, with the theory accurately describing the obtained cluster distributions in all cases. However, based on the strength and lifetime of associations in the simulated RTILs, we expect free ions to dominate ionic conductivity despite the presence of clusters, and we do not expect the percolating cluster to trigger structural arrest in the RTIL.

Introduction

Neat room temperature ionic liquids (RTILs) are electrolytes without any solvent: they are composed of molecular cations and anions that are sufficiently asymmetric and bulky to prevent solidification at room temperature.[1–5] RTILs are excellent solvents, have extremely low vapour pressures,[1–3] and are of great interest in energy storage devices because of their ability to withstand larger voltages without electrochemical decomposition.[4,6] However, owing to their high ionic concentrations and complicated molecular nature, *simple*, chemically-specific theoretical descriptions of RTILs have remained somewhat elusive.[7]

The conductivity of RTILs approximately follows that predicted by the Nernst-Einstein relation with some suppression factor. This has been interpreted as the ionicity of RTILs,[8,9] with the reduction factor being attributed to the presence of ion pairs in the system which do not contribute to conductivity.[10] In fact, pioneering molecular dynamics simulations of Feng *et al.*[11] investigated the role of ion clustering[12–14] in the conductivity, where it was found that "free" ions contribute the most.

Although the picture of RTILs as a mixture of ion pairs and free ions might be useful conceptually,[15–19] it is natural to question the validity of such a picture in such a highly concentrated system.[20] Surface force apparatus measurements performed in RTILs, when interpreted in terms of the DLVO theory, has reported extraordinary long screening lengths[21–23] consistent with $\ll 1\%$ of free ions.[22,23] While other methods of probing the number of free ions suggest significantly more free ions (15-25%) for common RTILs.[11,15,18] With such sig-

nificant degree of ion association, we would undoubtedly expect high order ionic clusters to be present.[11,24,25]

Thus, simple theoretical descriptions of RTILs beyond ion pairs are desired, but scarce. Recently Ref. 26 developed a thermodynamic theory of ion aggregation with arbitrary sized ionic clusters which predicted the emergence of a percolating ionic gel in super-concentrated electrolytes. It built off the theory of aggregation and gelation in polymer physics,[27–35] where clustering and percolation of aggregates is known to occur. Simulations of super-concentrated electrolytes have shown the presence of percolating ion networks.[36–38] Moreover, an elastic response has been measured in certain RTILs,[39,40,40–44] which can be indicative of the formation of a gel. Thus, it seems possible, if not probable, that extensive ion aggregation, and even gelation, is present in RTILs.

Here we study the limiting case of the theory established in Ref. 26: solvent-free RTILs modelled as an incompressible solution composed of solely ions. This naturally leads to a physically transparent framework of correlated ion-transport in RTILs, yielding coupled flux constitutive relations for diffusion and a modified Nernst-Eistein (NE) equation for ionic conductivity (also seen in Ref. 25). Our analysis allows us to determine the importance of clusters' contribution to ionic conductivity. We perform molecular dynamics (MD) simulations of 6 RTILs, and develop a general association criteria that is used to determine the cluster distribution of the simulated RTILs. From MD simulations, we determine the handful of parameters needed to compute the cluster distribution from our theory. We find the independently computed MD cluster distribution matches the theoretically computed distribution, with parameters derived from MD, extremely well (note we only compare quantities based off the cluster distribution between MD and theory - we do not investigate transport using MD here). Finally, we discuss our model's predictions of ion clustering and network formation as they pertain to ionic conduction and structural arrest in RTILs. In the Supporting Information (SI), we have a table of symbols, derivations of all equations and further details of the simulations.

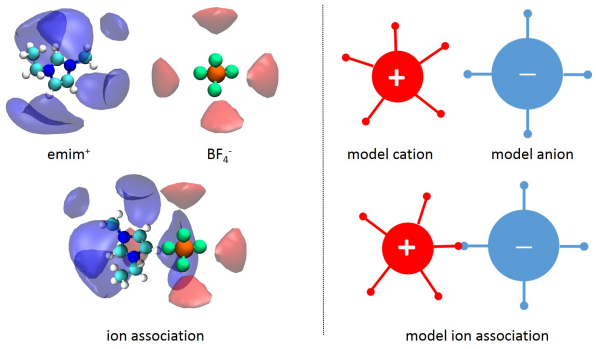

Figure 1: (Left) Schematic of example RTIL ions, emim^+ and BF_4^- with iso-density surface (corresponding to 2× the bulk density) of BF_4^- around emim^+, and emim^+ around BF_4^-. The former shows five distinct regions of preferred location for BF_4^- around emim^+ ($f_+ = 5$), and the latter four distinct regions of preferred location for emim^+ around BF_4^- ($f_- = 4$). Ionic associations, like the one shown in the bottom left, are formed when BF_4^- and emim^+ are found in each others high density regions (as seen by the iso-density surfaces which correspond to 2× the bulk density). (Right) A cartoon depicting the 'bonding' of cations and anions shown in the left panel.

Thermodynamics of Ion Clustering

We employ a Flory-like lattice fluid free energy of mixing[27] used extensively for polydisperse mixtures of thermoreversibly-associating polymer mixtures:[28–35]

$$\beta\Delta F = \sum_{lm} \left[N_{lm} \ln\left(\phi_{lm}\right) + N_{lm}\Delta_{lm}\right] + \Delta_+^{gel} N_+^{gel} + \Delta_-^{gel} N_-^{gel}. \tag{1}$$

Here $\beta = 1/k_B T$ is inverse thermal energy; N_{lm} and ϕ_{lm} are the number and volume fraction of lm clusters with l cations and m anions, respectively; Δ_{lm} is the free energy of formation of a rank lm cluster, which can have contributions from the combinatorial entropy, bonding energy, and configurational entropy; Δ_i^{gel} and N_i^{gel} are the free energy changes of i associating to the gel and number of i in the gel, respectively.[27,28,45] The free energy treats the electrolyte as an ideal mixture of non-interacting ionic clusters. In this way, the correlations beyond mean-field electrostatics are being treated via the formation of clusters. Our model does not account for correlations beyond the formation of clusters. Thus, our model relies on the assumption that the majority of the excess electrostatic energy of the mixture is modelled

via the formation of the ionic clusters.

The volume fraction of an ion cluster of rank lm is expressed by $\phi_{lm} = (l\xi_+ + m\xi_-)N_{lm}/\Omega$, where ξ_i is the volume of an ion relative to the volume of a lattice site and Ω denotes the total number of lattice sites (and is a proxy for the total volume of the mixture). The volume of a lattice site is arbitrary, and can either be taken to be the size of a cation, i.e. $\xi_+ = 1$ or an anion, i.e. $\xi_- = 1$. The system is considered to be incompressible (this is a reasonable approximation for RTILs, as the percentage of space occupied by voids is of the order of 10 %[46] at ambient conditions). A cation can associate to at most f_+ anions, and anions can associate to at most f_- cations. f_+ and f_- are referred to as functionalities of cations and anions, respectively. These functionalities are explained in more depth later.

The free energy is minimized by establishing equilibria between all ion clusters and free ions, as derived in the SI.[26] This process yields the following relation:

$$\phi_{lm} = K_{lm}\phi_{10}^{l}\phi_{01}^{m}, \tag{2}$$

where ϕ_{10} and ϕ_{01} are the volume fractions of free cations and anions, respectively, and the equilibrium constant is $K_{lm} = \exp(l + m - 1 - \Delta_{lm})$. The explicit form of Δ_{lm} was derived in Ref.,[26] and is detailed in the SI. It can be inserted into Eq. (2) yielding the thermodynamically consistent cluster distribution

$$\tilde{c}_{lm} = \frac{W_{lm}}{\lambda}\left(\lambda\psi_{10}\right)^{l}\left(\lambda\psi_{10}\right)^{m}. \tag{3}$$

where $\tilde{c}_{lm}$ is the dimensionless concentration of clusters of rank lm (# per lattice site), $\lambda = \exp(-\beta\Delta F_{+-})$ is the ionic association constant (derived explicitly in the SI) which depends on the free energy of ion association (ΔF_{+-}), $\psi_{10} = f_+\phi_{10}/\xi_+$ and $\psi_{01} = f_-\phi_{01}/\xi_-$ are the dimensionless concentrations of available bonding sites of cations and anions, respectively, and W_{lm} is the combinatorial multiplicity of lm clusters (number of different ways to form

a rank lm cluster), given by by[47]

$$W_{lm} = \frac{(f_+ l - l)!(f_- m - m)!}{l!m!(f_+ l - l - m + 1)!(f_- m - m - l + 1)!}. \tag{4}$$

In Eq. (3), $\tilde{c}_{lm}$ is written in terms of the volume fraction of free cations (ϕ_{10}) and anions (ϕ_{01}), but, in principle, ϕ_{10} and ϕ_{01} are unknown. We would like to know the distribution of clusters in terms of the overall volume fraction of species, ϕ_+ (volume fraction of cations) & ϕ_- (volume fraction of anions). We accomplish this by introducing ion association probabilities, p_{ij}, which is the probability that an association site of species i is bound to species j, where i and j in a binary RTIL correspond to cations (+) and anions (−). In this way, the volume fraction of free cations can be written as $\phi_{10} = \phi_+(1 - p_{+-})^{f_+}$ and free anions as $\phi_{01} = \phi_-(1 - p_{-+})^{f_-}$. Furthermore, we can determine the association probabilities through a conservation of associations

$$f_+ p_{+-} = f_- p_{-+} \tag{5}$$

and a mass action law between open and occupied association sites

$$\lambda\zeta = p_{+-}p_{-+}/(1 - p_{+-})(1 - p_{-+}), \tag{6}$$

where $\zeta = f_\pm p_{\pm\mp}\tilde{c}_{salt}$ is dimensionless concentration of associations with $\tilde{c}_{salt} = 1/(\xi_+ + \xi_-)$ denoting the dimensionless concentration of salt (# per lattice site). The definition of λ as the ionic *association constant* becomes clear from its appearance in the mass action law [Eq. (6)]. It sets the equilibrium for association sites to be occupied or open. Note, that even if $\lambda < 1$, it does not mean that associating clusters have an unfavorable energetic interaction. Precisely, a value of $\lambda < 1$ means that if an equimolar mixture of open and closed sites were introduce to each other the equilibrium would shift towards more open sites. The value of λ, itself would depend on both energetic and entropic contributions. Thus, even if the energy of

association is favorable, entropy can drive the association constant below one, as we describe in more detail later. Equations (5)&(6) close the system of equations in the pre-gel regime, and allows for the explicit calculation of cluster distribution.

If we assume that the RTIL is symmetrically associating ($f_+ = f_- = f$,$p_{+-} = p_{-+} = p$), then a *simple* analytical form can be obtained

$$p = \frac{1 + 2\tilde{c}_{salt} f\lambda - \sqrt{1 + 4\tilde{c}_{salt} f\lambda}}{2\tilde{c}_{salt} f\lambda}. \tag{7}$$

Analytical solutions for the asymmetric cases are written in the SI, which should be more typical for RTILs. For symmetric RTILs, the fraction of free ions, α, is simply

$$\alpha = \alpha_{01} + \alpha_{10} = \frac{\tilde{c}_{01} + \tilde{c}_{10}}{2\tilde{c}_{salt}} = \left[\frac{\sqrt{1 + 4\tilde{c}_{salt} f\lambda} - 1}{2\tilde{c}_{salt} f\lambda} \right]^f. \tag{8}$$

Here $\alpha_{01/10}$ are the fractions of free anions/cations, which are related to the dimensionless concentration of anions/cations through $1/2\tilde{c}_{salt}$. For large values of λ the fraction of free ions reduces to $\alpha = [2/\tilde{c}_{salt} f\lambda]^{f/2}$, which tends to zero.

If the functionalities of both ions are greater than 1 and the association probabilities exceed a certain threshold, then the RTIL can form a percolating ionic gel.[26] The criterion that determines this threshold can be seen plainly by examining the weight average degree of aggregation (the expected cluster size for a given ion), $\bar{n}$, can be expressed analytically as

$$\bar{n} = \frac{\sum_{lm} (l + m)^2 c_{lm}}{\sum_{lm} (l + m) c_{lm}} = \frac{1 + p}{1 - (f - 1)p}. \tag{9}$$

$\bar{n}$ diverges when $p^* = 1/(f - 1)$, which defines the gel point. This critical probability for gelation corresponds to a critical association strength for gelation of

$$\tilde{c}_{salt} \lambda^* = \frac{(f - 1)}{f(f - 2)^2}. \tag{10}$$

In the SI, we give the general critical association strength for asymmetrically associating ionic liquids. For $\lambda > \lambda^*$, the RTIL will form a gel. The critical association constant decreases as a function of f (for $f > 2$). Therefore, RTILs that can form more bonds with oppositely charged ions will tend to gel more readily. Note that the values of λ^* are practically always smaller than 1. This means that the gel phase will be present in ionic liquids even when the ion association constant favors open sites. The low threshold for gelation is largely a result of the high concentration of ions in RTILs, which pushes the equilibrium towards the formation of associations and eventually the gel. In fact, we see from Eq. (10), that the λ^* is inversely proportional to $\tilde{c}_{salt}$. Thus, for $\tilde{c}_{salt} \ll 1$, λ^* would have to be much larger than 1 in order to observe a percolating gel.

If the RTIL does form a gel, partitioning of species into the sol ($\phi_{\pm}^{sol}$) and gel ($\phi_{\pm}^{gel}$) phases must be performed and separate association probabilities for species in the sol ($p_{\pm\mp}^{sol}$) must be defined. These probabilities are determined from Flory's criterion that the free ion volume fractions can be written equivalently in terms of overall quantities and sol quantities.[48,49] The specific procedure associated with determining these probabilities is detailed explicitly in the SI.

Correlated Ion Transport

Our thermodynamic description treats RTILs as an ideal mixture of polydisperse ionic clusters. A consistent picture of ion transport would be independent diffusion of the ionic clusters. Of course, the assumption of independent cluster diffusion neglects the electrostatic interactions between clusters, which would inevitably result in molecular "friction" between clusters. However, as we have mentioned, the ionic associations between ions to form clusters should capture most of the electrostatic correlations beyond mean-field. Therefore, the simple presence of clusters results directly to strong correlations between ions, which is likely to dominate in strongly associated RTILs.

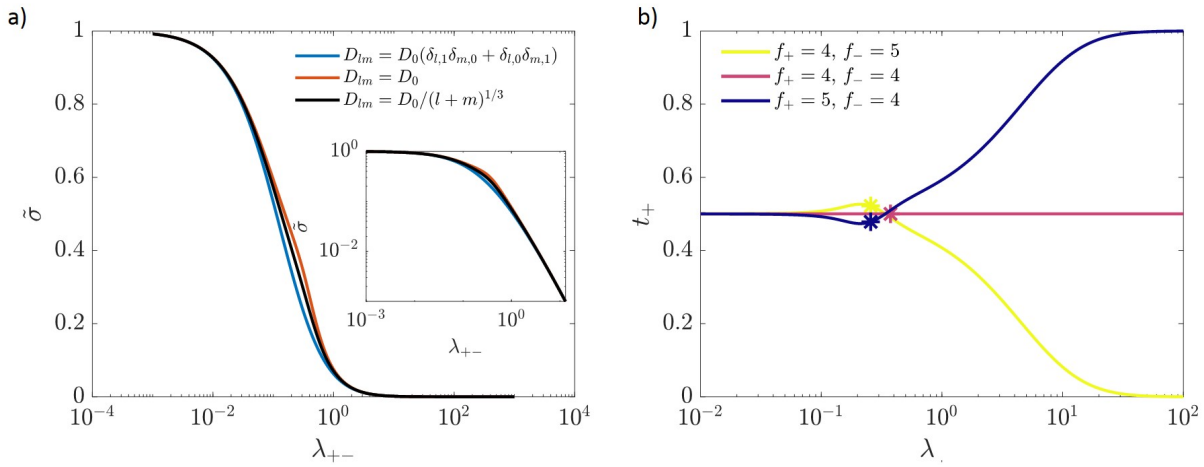

Figure 2: (a) Dimensionless ionic conductivity, $\tilde{\sigma}$, as a function of the ionic association constant, λ for $f = 4$. We use three different functional forms for the cluster diffusivity, D_{lm}, written in the legend of the left panel. In the inset, we plot the same curves on a log-log scale. (b) Cation transference number using Eq. (14), with $D_{lm} = D_0/(l+m)^{1/3}$, for various ion functionalities. The sums in Eq. (14) were cut off for clusters containing less than 16 ions ($l + m < 16$). The asterisks mark the gel point.

Another factor we must now consider is the lifetime of associations. From a thermodynamic point of view, ion cluster equilibrium is not *explicitly* dependent on the lifetimes of associations, as the equilibrium between clusters is permitted to be dynamic. The lifetimes of associations are important in terms of defining and computing the average thermodynamic properties of those associations. Thus, we can think of association lifetimes as *implicitly* influencing the thermodynamics of ion cluster equilibrium. However, for kinetic processes, like diffusion, the lifetime of a cluster will now play an important *explicit* role in understanding what clusters may contribute to the diffusive relaxation of the system. Principally, in order for a cluster to properly diffuse, the cluster must have a lifetime that is at least longer than than the velocity correlation time of the cluster,[11] which will be on the scale of the decay rate of the velocity auto-correlation function (VACF). As we will show, this may provide a size cut-off beyond which clusters will no longer contribute to overall ion diffusion.

Nonetheless, we may begin with the standard constitutive relation for diffusion that molar flux of a cluster of rank lm, $\mathbf{j}_{lm}$, is just simply proportional to the gradient of its

electrochemical potential, $\bar{\mu}_{lm}$

$$\mathbf{j}_{lm} = -\beta D_{lm} c_{lm} \nabla \bar{\mu}_{lm}, \tag{11}$$

where D_{lm} is the diffusivity of the rank lm cluster. Note that we have excluded the "$\sim$" on c_{lm}, as this is the concentration of clusters in terms of mole/volume as opposed to # per lattice site. The total flux of anions and cations can be computed by adding the contributions of all of the clusters ($\mathbf{j}_+ = \sum_{lm} l\mathbf{j}_{lm}$ & $\mathbf{j}_- = \sum_{lm} m\mathbf{j}_{lm}$).

The electrochemical potential of a rank lm cluster is simply $\bar{\mu}_{lm} = \mu_{lm} + e(l-m)\Psi$, where Ψ is the electrostatic potential. Moreover, assuming a local equilibrium among ion clusters, we may write the chemical potential of a rank lm cluster as $\mu_{lm} = l\mu_+ + m\mu_-$, where $\mu_\pm$ is the chemical potential of a (free) cation or anion. Writing the flux relations in matrix vector notation, also introducing the current density [$\mathbf{i} = e(\mathbf{j}_+ - \mathbf{j}_-)$], we have

$$\begin{bmatrix} \mathbf{j}_+ \\ \mathbf{j}_- \\ \mathbf{i} \end{bmatrix} = -2\beta c_{salt} \begin{bmatrix} \mathcal{D}_{++} & \mathcal{D}_{+-} & e(\mathcal{D}_{++} - \mathcal{D}_{+-}) \\ \mathcal{D}_{+-} & \mathcal{D}_{--} & e(\mathcal{D}_{--} - \mathcal{D}_{+-}) \\ e(\mathcal{D}_{++} - \mathcal{D}_{+-}) & e(\mathcal{D}_{+-} - \mathcal{D}_{--}) & e(\mathcal{D}_{++} - 2\mathcal{D}_{+-} + \mathcal{D}_{--}) \end{bmatrix} \begin{bmatrix} \nabla\mu_+ \\ \nabla\mu_- \\ \nabla\Psi \end{bmatrix} \tag{12}$$

where $\mathcal{D}_{++} = \sum_{lm} l^2 D_{lm}\alpha_{lm}$, $\mathcal{D}_{--} = \sum_{lm} m^2 D_{lm}\alpha_{lm}$, $\mathcal{D}_{+-} = \sum_{lm} lm D_{lm}\alpha_{lm}$ are binary diffusion coefficients, and $\alpha_{lm} = c_{lm}/2c_{salt}$ is the fraction clusters of rank lm. The binary diffusion coefficients are elements of the diffusivity tensor, $\underline{\underline{\mathcal{D}}}$, which is symmetric and positive-definite (via the Cauchy-Schwartz theorem) in accordance with the Onsager reciprocal relations.[50]

In the absence of chemical potential gradients, the ionic current is proportional to the gradient of the electrostatic potential via the ionic conductivity

$$\begin{aligned} \sigma &= 2e^2\beta c_{salt} \sum_{lm} (l-m)^2 \alpha_{lm} D_{lm} \\ &= 2e^2\beta c_{salt} (\mathcal{D}_{++} - 2\mathcal{D}_{+-} + \mathcal{D}_{--}) \end{aligned} \tag{13}$$

In the limit of all ions being free and the diffusion coefficient of the ions being related to the unimpeded diffusion of ions (Stokes-Einstein), one would predict a much larger conductivity than is observed in simulations and experiments.[11] Correlations between ions leads to the formation of clusters, which diminishes the concentration of free ions. Therefore, the ionic conductivity is reduced from the idealised NE relation in the presence of correlations, as has been well known for a long time in dilute electrolytes.

Similarly, the ion transference numbers, $t_{\pm}$, are defined as

$$t_+ = \frac{\sum_{lm} l(l-m)\alpha_{lm} D_{lm}}{\sum_{lm}(l-m)^2 \alpha_{lm} D_{lm}} = \frac{\mathcal{D}_{++} - \mathcal{D}_{+-}}{\mathcal{D}_{++} + \mathcal{D}_{--} - 2\mathcal{D}_{+-}} \tag{14}$$

for cations, and

$$t_- = \frac{\sum_{lm} m(l-m)\alpha_{lm} D_{lm}}{\sum_{lm}(l-m)^2 \alpha_{lm} D_{lm}} = \frac{\mathcal{D}_{--} - \mathcal{D}_{+-}}{\mathcal{D}_{++} + \mathcal{D}_{--} - 2\mathcal{D}_{+-}} \tag{15}$$

for anions. As we shall show, correlations between ions can give rise to large deviations of transference numbers between ions, provided some asymmetry is present in the system. Similar expressions (for conductivity and transference numbers) were recently proposed, though without the derivation shown here, in Refs. 25 and 26.

However, before going any further, we must elaborate on the effect of finite cluster lifetime. In Ref. 11, the diffusion of ions exchanging between dynamical states in typical RTILs was analyzed. It was shown that if the lifetime of ions in a state, simply considered to be "free" or "bound" in Ref. 11, is much larger than the velocity correlation time, then we may define independent diffusion coefficient for ions in those states. In terms of a cluster of rank lm, to define its independent diffusion coefficient we require the following inequality to be satisfied

$$\tau_{\nu,lm} < \tau_{lm} \tag{16}$$

where $\tau_{\nu,lm}$ and τ_{lm} are the velocity correlation time and lifetime of a cluster of rank lm, respectively. If the rank of the cluster is too large it will not obey Eq. (16), and thus will not contribute to the diffusive relaxation of the system because it will break apart before it can properly diffuse. The lifetime of a cluster of rank lm can be approximated as $\tau_{lm} = \tau_B / N_{B,lm}$,[51] where τ_B is the average lifetime of an ion association, and $N_{B,lm} = l+m-1$ is the total number of associations in a rank lm cluster because the clusters are assumed to form Cayley trees. Note that the lifetime of a cluster decreases with the total number of associations because only one association needs to break to destroy the cluster of rank lm. The velocity correlation time for a cluster of rank lm can be defined as $\tau_{\nu,lm} = \beta M_{lm} D_{lm}$,[11] where M_{lm} is the mass of a rank lm cluster. In order to solve for the conductivity, transference numbers, and each of the elements in $\underline{\underline{\mathcal{D}}}$, we must therefore specify D_{lm}, as well as τ_B. These are generally not known for RTILs, but we may inspect various scalings for D_{lm} as well as association lifetime to obtain qualitative predictions for the ionic conductivity and ion transference.

For example, a lower bound on the conductivity can be obtained if we assume that only free ions contribute, i.e. the diffusion constants of all other clusters are zero: $D_{lm} = D_0(\delta_{l,1}\delta_{m,0} + \delta_{m,1}\delta_{l,0})$, where D_0 is the self-diffusion coefficient of a free ion. Physically, this would correspond to a case when the lifetime of all clusters is shorter than the velocity correlation time for all associated clusters (ion pairs and greater), but where the lifetime of free ions is larger than their velocity correlation time.[11] In that case, the conductivity, non-dimensionalized by the factor, $2e^2\beta c_{salt} D_0$ (Nernst-Einstein conductivity), is simply given by

$$\tilde{\sigma}_{min} = \alpha = (1-p)^f \tag{17}$$

for the symmetrically associating RTIL (the asymmetric case is shown in the SI).

On the other hand, an upper bound can be obtained if we assume the diffusion constants

of all finite-sized clusters are that of a free ion ($D_{lm} = D_0$) and assume that the lifetimes of ion associations are infinite (such that $\tau_{lm} > \tau_{\nu,lm}$). This approximation yields the closed form

$$\tilde{\sigma}_{max} = \frac{1-p}{1+(f-1)p}. \tag{18}$$

for the symmetrically associating RTIL. Naturally, if a percolating gel cluster is formed, we assume it does not contribute to the conductivity even with this approximation, as the gel is infinite in size and could never physically obey Eq. (16) for finite life associations. Thus, when we surpass the critical gel point, we must use the sol probability, p^{sol} and multiply Eq. (18) by the fraction of the ions in the sol, $w_{\pm}^{sol} = \phi_{\pm}^{sol}/\phi_{\pm}$. For finite association lifetimes, it is clear that not all ionic clusters can contribute to conductivity. Indeed, within the assumption of $D_{lm} = D_0$ and assuming ions have equal masses ($M_+ = M_- = M$), Eq. (16) yields a finite cluster size constraint of

$$(l+m)(l+m-1) < \frac{\tau_B}{\tau_{\nu,0}} = \tilde{\tau}_B \tag{19}$$

where $\tau_{\nu,0}$ is the velocity correlation time of free ions given by $\beta M D_0$, and we have defined the dimensionless association lifetime, $\tilde{\tau}_B = \dfrac{\tau_B}{\tau_{\nu,0}}$.

In between these two approximations [Eqs. (17) & (18)], we can use the Stoke-Einstein scaling in which D_{lm} is inversely proportional to its radius, i.e. $D_{lm} = D_0/(l+m)^{1/3}$, which also provides a finite cut-off for cluster sizes. These assumptions yield the bounded series

$$\tilde{\sigma}_{mid} = \sum_{lm} \frac{(l-m)^2 \alpha_{lm}}{(l+m)^{1/3}}, \tag{20}$$

where the sum is over all l and m that satisfy Eq. (21), i.e. $\{l, m \mid \text{Eq. (21)}\}$. For this scaling, our constraint in Eq. (16) yields a cluster size cut-off of

$$(l+m)^{2/3}(l+m-1) < \tilde{\tau}_B \tag{21}$$

Thus, depending on the specific scaling expected for cluster diffusivity (D_{lm}), Eq. (16) can be used to generate transparent cluster size constraints, as we have shown with Eqs. (19) and (21). Timescales in literature are on the order of 1-100 ps for τ_B depending on the exact criteria for associations[10,52] and roughly 1 ps for $\tau_{\nu,0}$[11,12,52–56] (based on the decay time for the velocity auto-correlation function). Thus, $\tilde{\tau}_B$ could potentially vary from 1 to 100. Though as we discuss later in the text, simulations performed in this study suggest $\tilde{\tau}_B < 4$.

The conductivity approximations, $\tilde{\sigma}_{min}$, $\tilde{\sigma}_{max}$, and $\tilde{\sigma}_{mid}$, are plotted as a function of λ in Fig. 2 for symmetrically associating ions. For $\tilde{\sigma}_{mid}$ we cut the summation off for clusters containing less than 16 ions. This corresponds to dimensionless association lifetime of $\tilde{\tau}_B = 100$ [Eq. (21)]. We can see that as the strength of the ionic association parameter is increase, the conductivity monotonically decreases for all of the considered forms of D_{lm} and relative bond lifetimes. For very large association constants, we find a scaling of $\tilde{\sigma} \propto \lambda_{\pm}^{-f/2}$ for each of the models, owing to the conductivity being dominated by free ions when the RTIL has gelled significantly. Interestingly, we find that all three approximations for the cluster diffusion coefficients yield similar values of $\tilde{\sigma}$. The largest deviation between the models occurs around the gel point, as identifiable from the kink in the upper bound estimate. In Refs. 11, it was found that the free ions dominate the conductivity. We have demonstrated, through calculating the contributions from all clusters, that in fact, the free ions are always the dominant contribution.[26] Therefore, even if large charged clusters with infinite lifetimes exist in RTILs, they are not going to drastically alter the conductivity. The symmetrically associating RTIL approximation has a larger tendency to form neutral clusters, as opposed to charged ones. In the SI, we show additional examples of conductivity for various asymmetric RTILs, where charged clusters are more prevalent.

For the symmetric RTIL case, the transference numbers are trivially 1/2. Actually, many RTILs tend to have transference numbers close to 1/2 ($0.45 < t_{\pm} < 0.55$.[57,58] In the asymmetric case, however, our model predicts that transference numbers deviate from 1/2 dramatically, especially when there are large correlations between ions (large λ). Sure

enough, certain RTILs have been measured to have very asymmetric transference numbers ($t_\pm < 0.4$ or $t_\pm > 0.6$).[58]

In Fig. 2b we show how the cation transference number depends on λ for different cation functionalities [using Eq. (14), with $D_{lm} = D_0/(l+m)^{1/3}$]. Comments which follow apply to asymmetric functionalities, owing to the symmetric case being trivially 1/2. Prior to the gel point, the transference numbers tend to be close to 0.5, as there will be small concentrations of charged clusters and roughly equivalent dissociation of cations and anions. Close to the gel point, t_+ departs from 0.5 because the fraction of charged clusters drastically increases. For example, when $f_+ > f_-$, stoichiometry dictates that negatively charged clusters are formed more readily than positive clusters. These negative clusters drive $t_+ < 0.5$. When $f_+ < f_-$, the opposite is true. In the limit of the RTIL being significantly gelled ($\lambda \gg \lambda^*$), the transference number is governed by the fraction of free ions.[26] When $f_+ > f_-$, the gel will be negatively charged, meaning there will be more free cations than anions, and t_+ tends to 1.

The non-monotonic feature in t_+ seen in Fig. 2b will depend on the precise functional form of D_{lm} as well as the lifetime of associations. For example, as is shown in Fig. S4 (SI), we plot t_+ for a system with ion functionalities using $f_+ = 5$ and $f_- = 4$, for $D_{lm} = D_0(\delta_{l,1}\delta_{m,0} + \delta_{m,1}\delta_{l,0})$, $D_{lm} = D_0/(l+m)^{1/3}$, and $D_{lm} = D_0$. If the ion transference obeys the limit of solely free ion diffusion then the non-monotonicity disappears entirely. In the opposite limit, if clusters diffuse like free ions ($D_{lm} = D_0$) and satisfy the inequality in Eq. (19) then there is actually a singularity which arises in the transference number occurring at the gel point. Such singularity is not physical; diffusivity will undoubtedly strongly decrease as a function of cluster size, and Eq. (19) would ensure a finite cut-off for clusters that might contribute to ionic conduction.

One final note concerning our transport model is that in the post-gel regime there will be very few free ions[26] in a sea of ionic gel. In this case, it might be tempting to include a Kohlrausch-like correction[59] to their ionic mobility reflecting the long-range Coulomb in-

teractions between those free ions.[26] The ions, however, are not moving unimpeded between the clusters/gel, they inter-convert between the free and clustered states.[11] This is similar to electrons in intrinsic semiconductors that are thermally exited from valence to conduction band or of a solid electrolyte where there is a hopping mechanism for diffusion.[4,11] A Kohlrausch-like correction would not be justified for RTILs then, and the simple, 'single-particle' transport model of Eq. (13), which accounts for collective nature of transport trough the inter-conversion of ions between free and clustered states, would be the most natural starting point.

Comparison with Molecular Simulations

Given that our theory is derived from polymer physics,[28–35] it is reasonable to question if the model is representative of the microscopic behavior of RTILs, especially given that we have neglected an explicit treatment of electrostatic interactions between ions beyond ionic association.[26] To investigate this, we performed MD simulations of a number of representative imidazolium based RTILs at 295 K, and also studied the temperature dependence for one of the RTILs.

Imidazolium RTILs at Room Temperature

The first series of MD simulations performed included the following imidazolium RTILS: 1-Ethyl-3-methylimidazolium chloride (emimCl), 1-Ethyl-3-methylimidazolium bis(trifluoromethylsulfonyl) imide (emimTFSI), 1-Ethyl-3-methylimidazolium tetrafluoroborate (emimBF_4), 1-Ethyl-3-methylimidazolium hexafluorophosphate (emimPF_6), 1-Butyl-3-methylimidazolium hexafluorophosphate (bmimPF_6), and 1-Hexyl-3-methylimidazolium hexafluorophosphate (hmimPF_6). For specific details on the simulation, we direct the reader to the SI.

In order to compute the ion cluster distributions from MD simulations–independent of theory–we require a criterion for ion association. We need to find not only free ions, but

aggregates of all different ranks and sizes. In this case, a spatial criterion appears to be appropriate. The simplest spatial criterion would be a cutoff distance between the center of masses of cations and anions.[10,60] However, such a criterion does not account for the orientation of ions, or the directionality of specific interactions between functional groups, which mediate associations between ions.

In the left panel of Fig. 1, we display the spatial distribution functions (SDFs) of $emim^+$ and BF_4^-, which were generated by the open source software, TRAVIS.[61] In the SI, we show the computed SDFs for the other simulated RTIL ions. These SDFs are visualized as iso-density surfaces corresponding to regions where the density of counter-ions (based on centers of mass) are $2\times$ the average bulk density of counter-ions. They indicate "hot-spot" regions around ions where counter-ions are especially stable. These "hot-spot" regions, of which there are a well defined number, exist for RTIL ions because of their complicated molecular structure with de-localized charge, which gives rise to highly directional interactions, especially in ions that can hydrogen bond[62] or form interactions reminiscent of those in complex formation. This is in contrast to molten salts of highly concentrated inorganic salts, with highly localized charge, which would likely tend to form ordered semi-crystalline clusters rather than the branched, spatially-disordered clusters that RTIL ions form.[37,63] For molten salts, although ion clusters may indeed be present, the physical picture of clusters as prescribed by our model would not be entirely consistent with the strongly ordered, semi-crystalline clusters likely to comprise molten salts.

In order to capture the strong directionality of ionic associations in RTILs, we require that the center of mass of two associated ions mutually exist in each other's "hot-spots", as depicted in Fig. 1. Here, we choose a threshold iso-density value of $2\times$ the bulk density to define the "hot-spot" regions. In the SI we examine how ion association is affected by varying this threshold value. This ion-association criterion is advantageous because it is readily transferable between different RTILs, it can be used instantaneously for any MD snapshot, and it ensures that ions in close proximity have energetically favorable mutual

orientations with one another.

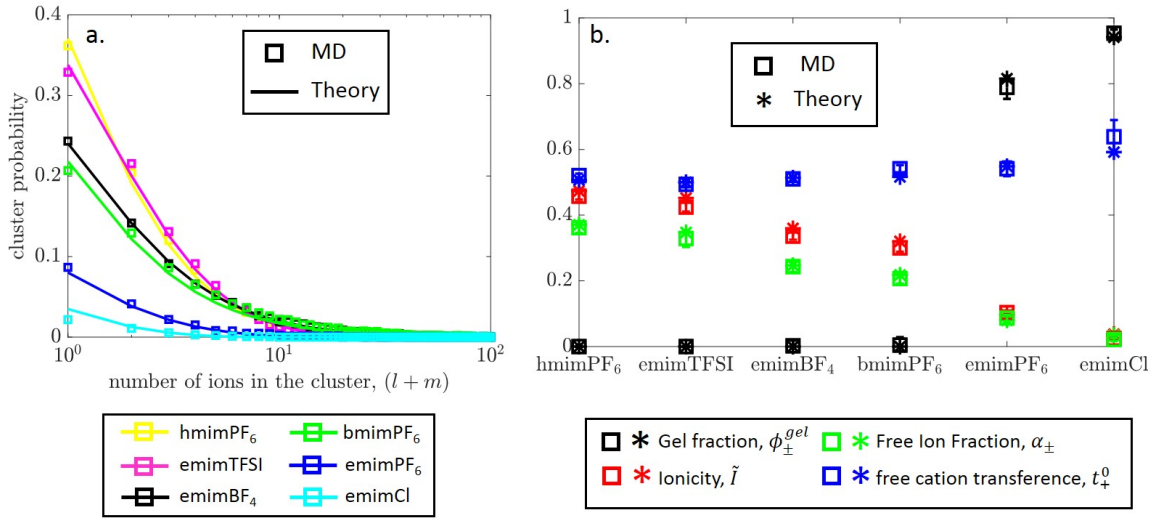

Figure 3: (a) Ionic cluster distributions for six RTILs at 295 K, as computed from MD (open squares) and theory (solid lines). (b) Gel fraction, ionicity [Eq. (23)], free ion fraction, and free cation transference number [t_+^0, Eq. (24)] are plotted for all six studied RTILs, with molecular dynamics values as open squares, and theoretical values as asterisks.

As we have alluded to, the SDF's for the ions displayed in Fig. 1 (further examples can be found in the SI), can also be used to determine the functionality of ions for our theory. For example, the SDF around the imidazolium cations (typically) show five distinct regions ($f_+ = 5$), which arise because of imidazolium ring is charged and planar, creating highly directional interactions with the anions; whereas the SDF around the BF_4- ion shows four distinct "hot-spot" regions on the faces of its tetrahedron molecular structure, indicating that it has a functionality of $f_- = 4$. The number of "hot-spots" itself does not always represent an ion's most apt functionality. For example, we observe eight distinct "hot-spots" on the PF_6^- ion, but we never observe more that 4 cations associated to a PF_6^- ion in our simulations, leading to our choice of $f_- = 4$ for PF_6^-. This is because imidazolium cations are bulky enough to block access to some additional "hot-spots" when they are associated to PF_6^-. Thus, an ion's functionality is determined by a combination of its number of "hot-spots", as well as the ability of the counter-ion to access those "hot-spots".

In order to compare the MD simulations to our theory we need to determine all theoretical

parameters. We explained above how ion functionality may be determined, so the only remaining parameters are $\tilde{c}_{salt}$ and λ, which may actually be grouped into a single parameter: $\Lambda = \lambda\tilde{c}_{salt}$, avoiding the additional complexity of computing λ and $\tilde{c}_{salt}$ individually. This final parameter can be determined with knowledge of the association probabilities and ion functionalities via the aforementioned mass action law in Eq. (6), rewritten as the following

$$\Lambda = \lambda\tilde{c}_{salt} = \frac{p_{-+}}{f_+(1-p_{+-})(1-p_{-+})} \tag{22}$$

where the ion association probability is computed from MD at each time step with simple definition: $p_{\pm\mp} = \#$ of associations/(# number of ions $\cdot$ $f_\pm$). The computed value of Λ is then ensemble averaged across all time steps. The parameters computed from MD simulations for our theory are reported in Tab. 1. It is interesting to note that the computed values of Λ were all computed to be smaller than 1 for the chosen threshold criterion for associations. However, this does not mean that clusters and associations are thermodynamically unstable. Rather, as we have said, Λ simply sets the equilibrium population of open vs. associated sites. Later, when we investigate the temperature dependence, the energetics of the associations are indeed found to be favorable. An interesting comparison can be made between the computed Λ values and the vacuum ion-pair and cohesive energies computed from ab-initio simulations performed in Ref. 64. Specifically, the vacuum ion-pair and cohesive energies display the same qualitative trend as Λ for emimPF_6, emimPF_6. and bmimPF_6: increasing alkyl chain length of the imidazolium cation leads to a decreased affinity to associate (smaller λ, and lower magnitude of ion pair and cohesive energy).

Overall, the cluster distribution from our theory, using parameters derived from the MD simulations, comes extremely close to the independently determined cluster distribution of the simulations, as seen in Fig. 3a. We observe the following trend in association affinity: emimCl > emimPF_6 > bmimPF_6 > emimBF_4 > emimTFSI > hmimPF_6. Moreover, we also explicitly plot various quantities in Fig. 3b, including gel fraction, ionicity, free ion fraction,

Table 1: Summary of Model Parameters at $T = 295$K

	Λ	f_+	f_-
hmimPF_6	0.07	5	4
emimTFSI	0.10	4	4
emimBF_4	0.11	5	4
bmimPF_6	0.13	5	4
emimPF_6	0.30	5	4
emimCl	0.54	5	4

and the free cation transference number. For all of these quantities, the model values nearly perfectly match those calculated from the performed MD simulations.

It is informative to compare ionicity–the dimensionless ionic strength–to the free ion fraction, because this highlights the potential importance (or not) of ionic clusters in the ionic strength of the electrolyte. Ionicity, $\tilde{I}$, is given by

$$\tilde{I} = \frac{1}{2}\sum_{lm}(l-m)^2\alpha_{lm}. \tag{23}$$

We see that for all RTILs, the free ion fractions are close to the ionicity. In fact, for emimPF_6 and emimCl the ionicity and free ion fractions are essentially indistinguishable. Whereas, for hmimPF_6, emimTFSI, emimBF_4, and bmimPF_6 there is a small, but noticeable difference between the ionicity and the free ion fraction.

Comparing the ionicity to the free ion fraction gives a measure of the presence of charged clusters, and therefore insight into the possibility of ionic current being carried by species other than free ions. We see that for all RTILs, the free ion fractions are close to the ionicity. This indicates that even if the association lifetime permits all clusters to contribute to the diffusive relaxation in the system, free ions would still be the primary contributor to ionic current in the observed RTILs. As will be discussed in detail later, accounting for the finite lifetimes of the associations places even more weight on the role of free ions in current conduction.

As seen in Fig. 3b, two of the RTILs, emimCl and emimPF_6, were found to have non-zero

gel fractions. It should be emphasized that our observation of percolating gel networks in emimCl and emimPF_6 (and lack gel in the other RTILs) depends heavily on our criterion for ionic association, specifically our iso-density threshold of 2× the bulk density. In the SI, we explore how varying this iso-density threshold changes the apparent association behavior of the RTIL, and we elaborate further on defining the gel in the simulations.

It has been suggested by Gebbie *et al.*[22,23] that RTILs behave as dilute electrolytes, with only 0.003% of ions being free, as discussed in the Introduction. If such a situation were true, our model predicts that the RTIL must be gelled. In fact, with such as small proportion of free ions, the system essentially only comprises of the gel phase and free ions.[26] This raises the questions of if the gel phase is playing a role in those surface-force measurements.

Finally, in Fig. 3b, we plot the free cation transference number, t_+^0, given by the following formula

$$t_+^0 = \frac{\alpha_+}{\alpha_+ + \alpha_-}, \tag{24}$$

which is essentially just the fraction of free ions that are cations. Note that t_+^0 is not a transport property. However, t_+^0 is related to the cation transference number, t_+, in the limit of free ion dominated conduction and equal cation and anion diffusivities.

If cations and anions have equivalent functionalities the theory predicts they should form positively and negatively charged clusters with equal probability and $t_+^0 = 0.5$. In general, when $f_+ > f_-$ (as is the case for the majority of RTILs studied here), the anions will have a larger probability to associate than cations. Thus, there will be more free cations than free anions, leading to $t_+^0 > 0.5$. However, for RTILs significantly below the gel point, the associations will not be abundant enough to drastically alter t_+^0 from 0.5, even if $f_+ \neq f_-$. For this reason, the majority of the RTILs studied were found to have t_+^0 very close to 0.5. However, for the most heavily associated RTIL that we simulated, emimCl, indeed we observe a significant positive deviation of t_+^0 from 0.5, with $t_+^0 = 0.65$, which is exactly in

line with our theoretical prediction.

The effect of ion functionality on ion transference could be more throroughly probed via its temperature dependence. Recall Fig. 2b, where t_+ is plotted as a function of the association constant λ. As intuitively expected and shown in the next section, λ will be a monotonically decreasing function of temperature. Thus, we can expect that when ion functionalities are equal, t_+ will not be a function of temperature, but rather fixed at a value set by the asymmetry in anion/cation diffusivity. However, when ion functionalities are unequal, t_+ will be a strong function of temperature. Of the six RTILs studied here, all but emimTFSI ($f_+ = 4, f_- = 4$) are expected to have a unequal functionalities ($f_+ = 5, f_- = 4$). Interestingly, ion transference numbers computed (from self-diffusion coefficients) for emimTFSI, emimPF_6, and bmimPF_6 in Ref. 10, as well as emimCl in Ref. 54 are all in qualitative agreement with the ion functionalities determined in this study. For example, the cation transference number of emimTFSI is relatively constant across a range of temperatures ranging from 350-500 K, whereas emimPF_6, bmimPF_6, and emimCl all strongly increase as temperature decreases. When $f_+ > f_-$, as determined for emimPF_6, bmimPF_6, and emimCl, the ratio of free cations to free anions will increase as a function of increasing λ or equivalently decreasing temperature. Thus, for free ion dominated conduction, t_+ would increase as a function of temperature for emimPF_6, bmimPF_6, and emimCl, but *not* emimTFSI.

We again emphasize the distinction between t_+^0 and t_+. t_+^0 does not take into account the ability of clusters to contribute ionic conduction, or asymmetric diffusion coefficients of free ions. Nonetheless, if the ion association lifetime prohibits the diffusive contribution of high order clusters, the transference number would be dominated by free ions, which in general have unequal diffusivity: $t_+ = \alpha_+ D_{+,0}/(\alpha_- D_{-,0} + \alpha_+ D_{+,0})$, where $D_{\pm,0}$ is the diffusivity of free cations/anions.

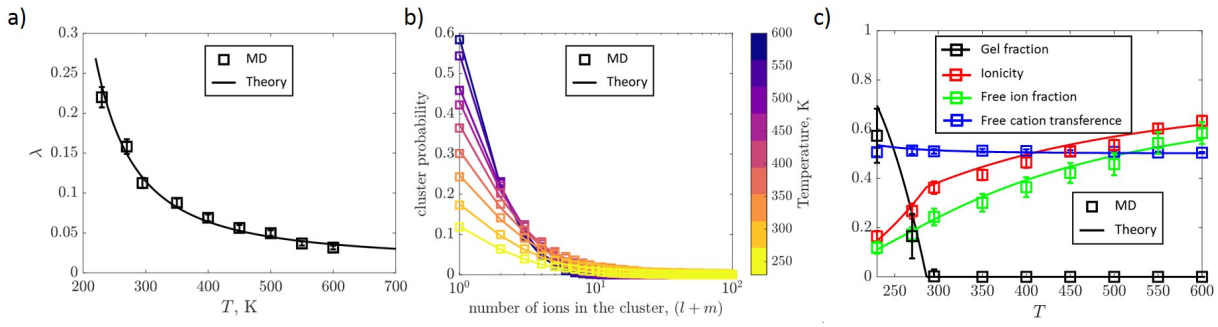

Figure 4: (a) Computed (from MD simulations of emimBF_4) ionic association constants, λ, as a function of temperature. The theoretical curve was generated via Eq. (25) by fitting to the simulation data. (b) Ionic cluster distribution (cluster probability as a function of size) for various temperatures ranging from 230-600 K. (c) Gel fraction, ionicity [Eq. (23)], and free ion fraction are plotted as a function of temperature.

Temperature dependence

In order to further probe our model, we performed a series of MD simulations of emimBF_4 at various temperatures (230-600 K). In Fig. 4a, we plot the computed λ values as a function of temperature. As we show in the SI, λ can be expressed as

$$\Lambda = \lambda \tilde{c}_{salt} = \frac{e^{-\beta(\Delta U_{+-} - T\Delta S_{+-})}}{\xi_+ + \xi_-}, \tag{25}$$

where ΔU_{+-} and ΔS_{+-} are the energy and entropy of association, respectively. The relative molecular volumes of $emim^+$ and BF_4^- give $\xi_+ = 2.4$ and $\xi_- = 1$, respectively. The solid curve in Fig. 4a, was generated from Eq. (25) with fitted values of $\Delta U_{+-} = -2.3 k_B T_0$ ($T_0 = 300$ K), and $\Delta S_{+-} = -3.3 k_B$. Thus, the ionic associations are driven by the exothermic energy of association, but at the cost of a strong decrease in entropy.

In Fig. 4b, we plot the cluster distribution of emimBF_4 for the studied temperatures, and once again we find quantitative agreement with the theory and simulations. Furthermore, in Fig. 4c we plot the ionicity, free ion fraction, gel fraction, and the free cation transference number as functions of temperature. Overall the theory agrees with the molecular simulations extremely well. Decreasing the temperature decreases both the ionicity and free ion fraction of emimBF_4, owing to the exothermic and entropy lowering nature of the ion

associations. We also see that a gel network forms in the simulation upon cooling below room temperature, but remember the gel transition temperature will depend strongly on the iso-density threshold used (2× the bulk density in Fig. 4). The free cation transference number stays roughly constant at 0.5 in decent agreement with the theory. Though, it would be expected to increase upon further reduction of the temperature.

Discussion

The comparison of our theory to the MD simulations give us a deeper understanding of the physical nature of RTILs as electrolytes. For one, it appears that, despite our neglect of explicit electrostatic interactions between ions beyond ionic associations, our theory performs exceptionally. We credit this to our previous statement that the majority of the electrostatic energy of the mixture is captured via the formation of the clusters. Excess contributions, such as the electrostatic interactions between ionic clusters, especially free ions, do not seem to strongly affect the cluster equilibria in RTILs.[26]

The success of our model in capturing the clustering for each of the simulated RTILs suggests that our treatment of the RTIL ions as simple poly-functional monomer units works effectively well. Furthermore, the temperature dependent study of ion clustering in emimBF_4 revealed to us the energetics of the ion associations, as well as the thermally reversible nature of the percolating ionic gel. Still there are some questions that remain. First, is the contribution of clusters to ionic current precluded by the limited lifetime of ionic associations? Second, will the emergence of a percolating ionic gel lead to structural arrest or "freezing" of an RTIL?

Ionic Conduction: Clusters or Free Ions?

A principal finding from studying the ionic clustering in emimBF_4 as a function of temperature was that we computed the energy of association to be only moderately exothermic

(-2.3 k_BT). This implies that the associations will frequently be broken via thermal excitations. Therefore, as we have previously alluded to, the lifetime of associations will be finite. As detailed in the SI, we find that the association lifetime (τ_B) ranges from 1-4 ps depending on the temperature (this is in good agreement with the range found by Ref. 52 but smaller than those found in Ref. 10). Based on the decay time velocity auto-correlation functions in many RTILs,[12,52–56] we expect $\tau_{\nu,0}$ to be approximately 1 ps. Using these scales for , τ_B and $\tau_{\nu,0}$, we would expect that $\tilde{\tau}_B < 4$. Thus, the constraints of Eq. (19) or (21) would only be satisfied by clusters containing only a few ions. For example, for $\tilde{\tau}_B = 4$, Eq. (21) gives a cluster cut-off of 3 ions, meaning that clusters larger than triplets would tend to break apart prior to the decay of the VACF, and thus not contribute to ion conduction. On the contrary, as is displayed in SI, the mean lifetime of free ions was found to be between 3-6 ps depending on the temperature; consistently longer than $\tau_{\nu,0}$. Therefore, we expect that free ions will undoubtedly contribute to ionic conduction in RTILs with small contributions from small ionic clusters, and likely no contribution from large ionic clusters. This is consistent with the observations by Gouveneur *et. al.*,[65] where the presence small asymmetric clusters were used to explain the observations of strongly asymmetric transference numbers in RTILs.

Thus, ion clustering plays two essential roles in affecting ion conductance and transference. First, clustering reduced the overall ionicity, and thus the mobile charge carriers in RTILs. This will result in a suppressed conductivity in RTILs. Second, as we have explained, when the ion functionalities are unequal, clusters will have a tendency to be charged (negatively for $f_- < f_+$ or positively for $f_- > f_+$). The non-zero net charge of clusters is necessarily balanced by the unequal fraction of free anions vs cations. Thus, in the expected case of a free-ion dominated ionic current, the asymmetry in free ion fraction would correspond directly to an asymmetry in ion transference.

It has been found in a number of studies, that a certain fraction of ions in RTILs propagate freely for a time significantly longer than the bonding lifetime.[12–14] Indeed, in Ref. 11 it was shown that these free ions are the dominant contributor to ionic current. Our results

agree with those quite well. Having said this, the precise contribution (or lack there of) of clusters to the ionic current will depend strongly on the association lifetime, which is highly dependent on the iso-density threshold and the scaling used to derive Eqs. (21) & (21). Nonetheless, our conclusion still remains that ionic conduction is principally governed by free ion diffusion. Other RTILs may have associations with longer lifetimes than those studied here,[10] but likely not long enough to substantially change our conclusion. On the other hand, RTIL systems containing lithium or other small alkali cations will likely have much stronger associations than those in ordinary RTILs with organic cations, making the expected lifetimes of associations much longer.[66,67] In these cases, ion clusters may indeed play a much larger role in the diffusive relaxation of the system. There is specific proof of this in Refs. 68–71, where sodium ions and lithium ions were found to have negative transference numbers when dissolved in RTILs at low concentrations. This type of phenomenon is something that can be readily explained by the vehicular transport of sodium and lithium in longer-lived, net-negative clusters.

Structural Arrest: Gelation or Glass Transition?

The thermodynamic theory, in addition to the molecular simulations, presented here suggests that a percolating ionic gel could form in RTILs around room temperature.[5,20,26,72] Additionally, a number of other simulation studies[70,73] indicate that a percolating cluster may be present in RTILs depending on the temperature and association criteria. The existence of a percolating cluster in RTILs is thus not completely unexpected. However, we now must discuss the implications of such a cluster.

Throughout this article, we have defined gelation as the appearance of a percolating cluster, as is consistent with gelation in thermoreversibly associating polymer systems. Yet, as noted by Kumar and Douglas,[74] gelation stems from a latin word meaning "to freeze". Thus it is natural to consider if the RTIL will acquire solid-like properties when a percolating cluster is present. In chemical gels it is well known that bond percolation is accompanied

by a rheological transition, leading to a power-law divergence of viscosity and emergence of elasticity,[75] i.e. the mixture gains solid-like properties. There is a direct analogy between chemical and thermoreversible gels, but typically this analogy holds only for timescales less than the characteristic association lifetime.[76,77] Thus, it appears that the observed percolating clusters would only confer solid-like properties upon the RTIL for very short time scales.

A conceptually similar phenomenon to gelation is the glass transition. The glass transition is characterized by the kinetic arrest of molecules, physically similar to freezing. However, glassy systems lack the long range order typically found in solids. Interestingly, imidazolium RTILs are known fragile glass-formers,[5,78,79] where an liquid's fragility correlates with how rapidly it undergoes the glass transition. This is actually entirely consistent with our finding that association in emimBF_4 are inflexible (as determined by the strong negative entropy of association). It is well-established that the stiffness or lack of flexibility in molecular chains leads to glass transitions in polymeric systems.[80] In fact, connections of the glass transition to thermodynamics[81–83] suggest a correlation between the configurational entropy landscape of a liquid and its the fragility. Thus, the thermodynamics, specifically the configurational entropy, of ionic associations could be of principal importance for understanding how and why glass transitions occur in RTILs.

Furthermore, the success of our model in capturing the cluster distributions observed by simulations suggests a strong connection between RTILs and the well-studied patchy particle systems in Refs.[74,84–92] These are systems of model particles with have limited valence, highly directional interactions, i.e. they have fixed functionalities analogous to our model that are representative of colloidal systems. The general consensus from these works is that the presence of a percolating cluster is generally only accompanied by structural arrest if the associations are strong/long-lived and the system is not so concentrated that the physical effects of percolation are masked by the glass transition. Furthermore, concentrated systems of weakly associating patchy particles were found to share much of the dynamical behavior

of fragile-glass forming systems,[74] once again corroborating the connection of these systems to RTILs.

Thus, the weakly-exothermic energy, short lifespan, strong entropic cost of associations, in addition to the overly high concentration of ions in RTILs, clearly suggest that gelation/percolation will not be accompanied by structural arrest for the studied RTILS, and solid-like transitions in RTILs are more likely the result of the glass transition. Percolation would undoubtedly be expected to precede the glass transition and could serve as an upward bound for the start of vitrification in RTILs.

While the percolation threshold predicted by our theory may not indicate a stark transition in physical properties of RTILs or their structural arrest, the presence of the percolating networks are consistent and can help explain the structural organization in RTILs.[20,93] The emergence of such mesoscopic nanostructure in RTILS is attributed in large part to the amphiphilic character of the RTIL ions. For example, imidazolium cations contain non-polar/hydrophobic, hydrocarbon tails and polar/hydrophilic, aromatic heads. Conversely, many RTIL anions, such as the ones studied here, tend to have more localized charge and are thus more hydrophilic. The MD simulations performed in Ref. 93 showed that the polar heads of cations form a continuous, 3-dimensional network with the anions that excludes the hydrocarbon tails. This type of phenomenon would be exactly represented by the emergence of a percolating cluster that is bridged by the directional interactions between anions and cations as we have defined in this work. Observing the SDFs in Fig. 8 of the SI, we see that the imidazolium hot-spots are localized around the aromatic head of the ion, while the hot-spots are more evenly spaced around the anions. Thus, associations bridged by these hot-spots would exclude the hydrocarbon tails, and the emergence of a percolating cluster would indeed create a 3-dimensional continuous network containing the polar groups in the RTIL.

Furthermore, additives to RTILs could trigger percolation/gelation induced structural arrest. As we have mentioned, the dissolution of alkali salts in RTILs leads to clusters

strongly affecting the transport of the alkali cation. The percolation of the alkali salt clusters within the RTIL is expected from simulation,[69,70] and contain associations that are strong enough to arrest the system as in traditional gelation processes.[94] Furthermore, additives to RTILs other than alkali salts (such as water,[73,95,96] acetonitrile,[97] or "gelator molecules"[42,98]), show the presence of a gel phase upon their addition. These observations suggest that RTIL *mixtures* are capable of gelation, even if it is not detectable in their neat formulations.

Conclusion

In this article, we outlined a simple, general theory for the formation of arbitrarily large ionic clusters and the onset of a percolating infinite cluster (gel) in room temperature ionic liquids (RTILs). Using the developed thermodynamics of ion clustering, we constructed a simple theory of coupled fluxes directly resulting from the presence of charged clusters in RTILs. Such a theory is much needed for RTILs, for which the idealized picture of ion pairs is perhaps too simplified. Recently, in Ref. 7, the development of "chemically specific theories" was identified as a key challenge for guiding electrolyte design in the next generation of battery electrolytes. Our model responds to this challenge. In particular, it was was able to capture some molecular specificity via the association constant (λ) and ion functionality parameters ($f_{\pm}$).

We performed molecular dynamics (MD) simulations of six RTILs. From the spatial distribution functions of bulk simulations, we developed a general association criteria for ions based off their relative positions and orientations. This allowed the cluster distributions to be obtained from MD simulations. The parameters required for the theory are the ion functionalities and the strength of their association. As we outlined in detail, these can be independently determined from MD and used in the theory, resulting in agreement between the theoretical and MD cluster distributions for all studied RTILs.

The comparison between the MD simulations and the theory provided valuable insight.

For one, our model's treatment of RTIL ions as simple, poly-functional, associative monomer units reproduced the observed cluster distributions for all of the simulated RTILs. The The temperature dependence of association allowed us to compute the association energy and entropy in emimBF_4. Interestingly, the energy of association was found to be weakly exothermic ($-2.3k_BT$), indicating that associations will likely be relatively short-lived breaking frequently due to thermal excitation. The somewhat weak and ephemeral nature of the associations indicates that large clusters will not live long enough to contribute significantly to ionic conduction, and the percolating cluster (gel) will not lead to a lasting structural arrest of the RTIL. Additionally, it was found that there is a strong negative entropy of association (-3.3k_B) in emimBF_4 indicating that associations in RTILs are very stiff. Association stiffness is a known to induce glass transitions via the "entropy catastrophy" in polymer systems[80] and could likely induce glass transitions in RTILs as well.

Some experimental signatures of clustering and percolation in RTILs have been previously reported, as we highlighted, and we believe that the presented theory should guide further experimental work on the extent and effects of clustering and percolation in RTILs. We expect that such a theory may be extended to more complex ionic mixtures,[99] such as polymer-based semi-solid electrolytes[100] or perhaps even super-concentrated electrolyte mixtures with multiple salts [69,70,101–104] or multiple solvents.[71,105–108]

Supporting Information

Table of symbols; derivation of cluster distribution; derivations of equations for asymmetrically associating RTILS (association probabilities, gel point, and conductivity); definition of gel from simulations; results obtained with variable iso-density threshold; simulation details.

Acknowledgements

All authors would like to acknowledge the Imperial College-MIT seed fund. MM and MZB acknowledge support from a Amar G. Bose Research Grant. ZG was supported through a studentship in the Centre for Doctoral Training on Theory and Simulation of Materials at Imperial College London funded by the EPSRC (EP/L015579/1) and from the Thomas Young Centre under grant number TYC-101. AK would like to acknowledge the research grant by the Leverhulme Trust (RPG-2016- 223). This work used the Extreme Science and Engineering Discovery Environment (XSEDE), which is supported by National Science Foundation grant number ACI-1548562.

References

(1) Hallett, J. P.; Welton, T. Room-Temperature Ionic Liquids: Solvents for Synthesis and Catalysis. 2. *Chem. Rev.* **2011**, *111*, 3508–3576.

(2) Welton, T. Room-Temperature Ionic Liquids. Solvents for Synthesis and Catalysis. *Chem. Rev.* **1999**, *99*, 2071–2083.

(3) Wasserscheid, P.; Welton, T. *Ionic liquids in synthesis*; John Wiley & Sons, 2008.

(4) Fedorov, M. V.; Kornyshev, A. A. Ionic Liquids at Electrified Interfaces. *Chem. Rev.* **2014**, *114*, 2978–3036.

(5) Weingärtner, H. Understanding Ionic Liquids at the Molecular Level: Facts, Problems, and Controversies. *Angew. Chem. Int.* **2008**, *47*, 654–670.

(6) Kondrat, S.; Kornyshev, A. A. Pressing a spring: what does it take to maximize the energy storage in nanoporous supercapacitors? *Nanoscale Horiz.* **2016**, *1*, 45–52.

(7) Son, C. Y.; Wang, Z.-G. Ion transport in small-molecule and polymer electrolytes. *J. Chem. Phys.* **2020**, *153*, 100903.

(8) MacFarlane, D. R.; Forsyth, M.; Izgorodina, E. I.; Abbott, A. P.; Annata, G.; Fraser, K. On the concept of ionicity in ionic liquids. *Phys. Chem. Chem. Phys.* **2009**, *11*, 4962–4967.

(9) Hollóczki, O.; Malberg, F.; Welton, T.; Kirchner, B. On the origin of ionicity in ionic liquids. Ion pairing versus charge transfer. *Phys. Chem. Chem. Phys.* **2014**, *16*, 16880–16890.

(10) Zhang, Y.; Maginn, E. J. Direct Correlation between Ionic Liquid Transport Properties and Ion Pair Lifetimes: A Molecular Dynamics Study. *J. Phys. Chem. Lett.* **2015**, *6*, 700–705.

(11) Feng, G.; Chen, M.; Bi, S.; Goodwin, Z. A. H.; Postnikov, E. B.; Brilliantov, N.; Urbakh, M.; Kornyshev, A. A. Free and Bound States of Ions in Ionic Liquids, Conductivity, and Underscreening Paradox. *Phys. Rev. X* **2019**, *9*, 021024.

(12) Pópolo, M. G. D.; Voth, G. A. On the Structure and Dynamics of Ionic Liquids. *J. Phys. Chem. B* **2004**, *108*, 1744–1752.

(13) Araque, J. C.; Yadav, S. K.; Shadeck, M.; Maroncelli, M.; Margulis, C. J. How Is Diffusion of Neutral and Charged Tracers Related to the Structure and Dynamics of a Room-Temperature Ionic Liquid? Large Deviations from Stokes–Einstein Behavior Explained. *J. Phys. Chem. B* **2015**, *119*, 7015–7029.

(14) Hu, Z.; Margulis, C. J. Heterogeneity in a room-temperature ionic liquid: Persistent local environments and the red-edge effect. *Proc. Natl. Acad.Sci.* **2006**, *103*, 831–836.

(15) Lee, A. A.; Vella, D.; Perkin, S.; Goriely, A. Are room-temperature ionic liquids dilute electrolytes? *J. Phys. Chem. Lett.* **2014**, *6*, 159–163.

(16) Goodwin, Z. A.; Kornyshev, A. A. Underscreening, overscreening and double-layer capacitance. *Electrochem. Commun.* **2017**, *82*, 129–133.

(17) Goodwin, Z. A.; Feng, G.; Kornyshev, A. A. Mean-field theory of electrical double layer in ionic liquids with account of short-range correlations. *Electrochim. Acta* **2017**, *225*, 190–197.

(18) Chen, M.; Goodwin, Z. A. H.; Feng, G.; Kornyshev, A. A. On the temperature dependence of the double layer capacitance of ionic liquids. *J. Electroanal. Chem.* **2018**, *819*, 347–358.

(19) Adar, R. M.; Markovich, T.; Andelman, D. Bjerrum pairs in ionic solutions: A Poisson-Boltzmann approach. *J. Chem. Phys.* **2017**, *146*, 194904.

(20) Hayes, R.; Warr, G. G.; Atkin, R. Structure and Nanostructure in Ionic Liquids. *Chem. Rev.* **2015**, *115*, 6357–6426.

(21) Smith, A. M.; Lee, A. A.; Perkin, S. The Electrostatic Screening Length in Concentrated Electrolytes Increases with Concentration. *J. Phys. Chem. Lett.* **2016**, *7*, 2157–2163.

(22) Gebbie, M. A.; Valtiner, M.; Banquy, X.; Fox, E. T.; Henderson, W. A.; Israelachvili, J. N. Ionic liquids behave as dilute electrolyte solutions. *Proc. Natl. Acad. Sci. U.S.A* **2013**, *110*, 9674–9679.

(23) Gebbie, M. A.; Dobes, H. A.; Valtiner, M.; Israelachvili, J. N. Long-range electrostatic screening in ionic liquids. *Proc. Natl. Acad. Sci. U.S.A* **2015**, *112*, 7432–7437.

(24) Avni, Y.; Adar, R. M.; Andelman, D. Charge oscillations in ionic liquids: A microscopic cluster model. *Phys. Rev. E* **2020**, *101*, 010601.

(25) France-Lanord, A.; Grossman, J. C. Correlations from ion pairing and the Nernst-Einstein equation. *Phys. Rev. Lett.* **2019**, *122*, 136001.

(26) McEldrew, M.; Goodwin, Z. A.; Bi, S.; Bazant, M. Z.; Kornyshev, A. A. Theory of Ion

Aggregation and Gelation in Super-Concentrated Electrolytes. *J. Chem. Phys.* **2020**, *152*, 234506.

(27) Flory, P. J. Thermodynamics of high polymer solutions. *J. Chem. Phys.* **1942**, *10*, 51–61.

(28) Tanaka, F. Theory of thermoreversible gelation. *Macromolecules* **1989**, *22*, 1988–1994.

(29) Tanaka, F. Thermodynamic theory of network-forming polymer solutions. 1. *Macromolecules* **1990**, *23*, 3784–3789.

(30) Tanaka, F.; Stockmayer, W. H. Thermoreversible gelation with junctions of variable multiplicity. *Macromolecules* **1994**, *27*, 3943–3954.

(31) Tanaka, F.; Ishida, M. Thermoreversible gelation of hydrated polymers. *J. Chem. Soc. Faraday Trans.* **1995**, *91*, 2663–2670.

(32) Ishida, M.; Tanaka, F. Theoretical study of the postgel regime in thermoreversible gelation. *Macromolecules* **1997**, *30*, 3900–3909.

(33) Tanaka, F. Thermoreversible gelation of associating polymers. *Physica A: Statistical Mechanics and its Applications* **1998**, *257*, 245–255.

(34) Tanaka, F.; Ishida, M. Thermoreversible gelation with two-component networks. *Macromolecules* **1999**, *32*, 1271–1283.

(35) Tanaka, F. Theoretical study of molecular association and thermoreversible gelation in polymers. *Polym. J.* **2002**, *34*, 479.

(36) Borodin, O.; Suo, L.; Gobet, M.; Ren, X.; Wang, F.; Faraone, A.; Peng, J.; Olguin, M.; Schroeder, M.; Ding, M. S., et al. Liquid structure with nano-heterogeneity promotes cationic transport in concentrated electrolytes. *ACS Nano.* **2017**, *11*, 10462–10471.

(37) Choi, J.-H.; Lee, H.; Choi, H. R.; Cho, M. Graph theory and ion and molecular aggregation in aqueous solutions. *Annu. Rev. Phys. Chem.* **2018**, *69*, 125–149.

(38) Jeon, J.; Lee, H.; Choi, J.-H.; Cho, M. Modeling and Simulation of Concentrated Aqueous Solutions of LiTFSI for Battery Applications. *J. Phys. Chem. C* **2020**,

(39) Makino, W.; Kishikawa, R.; Mizoshiri, M.; Takeda, S.; Yao, M. Viscoelastic properties of room temperature ionic liquids. *J. Chem. Phys.* **2008**, *129*, 104510.

(40) Tao, R.; Simon, S. L. Rheology of imidazolium-based ionic liquids with aromatic functionality. *J. Phys. Chem. B* **2015**, *119*, 11953–11959.

(41) Elhamarnah, Y. A.; Nasser, M.; Qiblawey, H.; Benamor, A.; Atilhan, M.; Aparicio, S. A comprehensive review on the rheological behavior of imidazolium based ionic liquids and natural deep eutectic solvents. *J. Mol. Liq.* **2019**, *277*, 932—-958.

(42) Shakeel, A.; Mahmood, H.; Farooq, U.; Ullah, Z.; Yasin, S.; Iqbal, T.; Chassagne, C.; Moniruzzaman, M. Rheology of Pure Ionic Liquids and Their Complex Fluids: A Review. *ACS Sustainable Chem. Eng.* **2019**, *7*, 13586–13626.

(43) Shamim, N.; McKenna, G. B. Glass Dynamics and Anomalous Aging in a Family of Ionic Liquids above the Glass Transition Temperature. *J. Phys. Chem. B* **2010**, *114*, 15742–15752.

(44) Choi, U. H.; Ye, Y.; de la Cruz, D. S.; Liu, W.; Winey, K. I.; Elabd, Y. A.; Runt, J.; Colby, R. H. Dielectric and Viscoelastic Responses of Imidazolium-Based Ionomers with Different Counterions and Side Chain Lengths. *Macromolecules* **2014**, *47*, 777–790.

(45) Flory, P. J. *Principles of polymer chemistry*; Cornell University Press, 1953.

(46) Yu, Y.; Beichel, W.; Dlubek, G.; Krause-Rehberg, R.; Paluch, M.; Pionteck, J.; Pfefferkorn, D.; Bulut, S.; Friedrich, C.; Pogodina, N., et al. Free volume and phase

transitions of 1-butyl-3-methylimidazolium based ionic liquids from positron lifetime spectroscopy. *Phys. Chem. Chem. Phys.* **2012**, *14*, 6856–6868.

(47) Stockmayer, W. H. Molecular distribution in condensation polymers. *J. Polym. Sci.* **1952**, *9*, 69–71.

(48) Flory, P. J. Molecular size distribution in three dimensional polymers. I. Gelation1. *J. Am. Chem. Soc.* **1941**, *63*, 3083–3090.

(49) Flory, P. J. Molecular size distribution in three dimensional polymers. II. Trifunctional branching units. *J. Am. Chem. Soc.* **1941**, *63*, 3091–3096.

(50) Onsager, L. Reciprocal relations in irreversible processes. I. *Phys. Rev.* **1931**, *37*, 405.

(51) Winter, H. H.; Mours, M. *Neutron spin echo spectroscopy viscoelasticity rheology*; Springer, 1997; pp 165–234.

(52) Kirchner, B.; Malberg, F.; Firaha, D. S.; Hollóczki, O. Ion pairing in ionic liquids. *J. Phys.: Condens. Matter* **2015**, *27*, 463002.

(53) Bhargava, B.; Balasubramanian, S. Dynamics in a room-temperature ionic liquid: A computer simulation study of 1, 3-dimethylimidazolium chloride. *J. Chem. Phys.* **2005**, *123*, 144505.

(54) Rey-Castro, C.; Vega, L. F. Transport properties of the ionic liquid 1-ethyl-3-methylimidazolium chloride from equilibrium molecular dynamics simulation. The effect of temperature. *J. Phys. Chem. B* **2006**, *110*, 14426–14435.

(55) Liu, H.; Maginn, E. A molecular dynamics investigation of the structural and dynamic properties of the ionic liquid 1-n-butyl-3-methylimidazolium bis (trifluoromethanesulfonyl) imide. *J. Chem. Phys.* **2011**, *135*, 124507.

(56) Kashyap, H. K.; Annapureddy, H. V.; Raineri, F. O.; Margulis, C. J. How is charge transport different in ionic liquids and electrolyte solutions? *J. Phys. Chem. B* **2011**, *115*, 13212–13221.

(57) Galiński, M.; Lewandowski, A.; Stepniak, I. Ionic liquids as electrolytes. *Electrochim. Acta* **2006**, *51*, 5567–5580.

(58) Kowsari, M.; Alavi, S.; Ashrafizaadeh, M.; Najafi, B. Molecular dynamics simulation of imidazolium-based ionic liquids. I. Dynamics and diffusion coefficient. *J. Chem. Phys.* **2008**, *129*, 224508.

(59) Fuoss, R. M.; Onsager, L. Conductance of Unassociated Electrolytes. *J. Phys. Chem.* **1957**, *61*, 668–682.

(60) Levy, A.; McEldrew, M.; Bazant, M. Z. Spin-glass charge ordering in ionic liquids. *Phys. Rev. Mater* **2019**, *3*, 055606.

(61) Brehm, M.; Kirchner, B. TRAVIS-a free analyzer and visualizer for Monte Carlo and molecular dynamics trajectories. *J. Chem. Inf. Model.* **2011**, *51*, 2007–2023.

(62) Hunt, P. A.; Ashworth, C. R.; Matthews, R. P. Hydrogen bonding in ionic liquids. *Chem. Soc. Rev.* **2015**, *44*, 1257.

(63) Dupont, J. From molten salts to ionic liquids: a "nano" journey. *Acc. Chem. Res.* **2011**, *44*, 1223–1231.

(64) McDaniel, J. G.; Choi, E.; Son, C. Y.; Schmidt, J.; Yethiraj, A. Ab initio force fields for imidazolium-based ionic liquids. *J. Phys. Chem. B* **2016**, *120*, 7024–7036.

(65) Gouverneur, M.; Kopp, J.; van Wüllen, L.; Schönhoff, M. Direct determination of ionic transference numbers in ionic liquids by electrophoretic NMR. *Phys. Chem. Chem. Phys.* **2015**, *17*, 30680–30686.

(66) Diaw, M.; Chagnes, A.; Carre, B.; Willmann, P.; Lemordant, D. Mixed ionic liquid as electrolyte for lithium batteries. *J. Power Sources* **2005**, *146*, 682–684.

(67) Seki, S.; Ohno, Y.; Kobayashi, Y.; Miyashiro, H.; Usami, A.; Mita, Y.; Tokuda, H.; Watanabe, M.; Hayamizu, K.; Tsuzuki, S., et al. Imidazolium-based room-temperature ionic liquid for lithium secondary batteries: Effects of lithium salt concentration. *J. Electrochem. Soc.* **2007**, *154*, A173.

(68) Gouverneur, M.; Schmidt, F.; Schönhoff, M. Negative effective Li transference numbers in Li salt/ionic liquid mixtures: does Li drift in the "Wrong" direction? *Phys. Chem. Chem. Phys.* **2018**, *20*, 7470–7478.

(69) Molinari, N.; Mailoa, J. P.; Kozinsky, B. General Trend of a Negative Li Effective Charge in Ionic Liquid Electrolytes. *J. Phys. Chem. Lett.* **2019**, *10*, 2313–2319.

(70) Molinari, N.; Mailoa, J. P.; Craig, N.; Christensen, J.; Kozinsky, B. Transport anomalies emerging from strong correlation in ionic liquid electrolytes. *J. Power Sources* **2019**, *428*, 27–36.

(71) Molinari, N.; Kozinsky, B. Chelation-Induced Reversal of Negative Cation Transference Number in Ionic Liquid Electrolytes. *J. Phys. Chem. B* **2020**, *124*, 2676–2684.

(72) Dupont, J. On the Solid, Liquid and Solution Structural Organization of Imidazolium Ionic Liquids. *J. Braz. Chem. Soc.* **2004**, *3*, 341–350.

(73) Bernardes, C. E. S.; da Piedade, M. E. M.; Lopes, J. N. C. The Structure of Aqueous Solutions of a Hydrophilic Ionic Liquid: The Full Concentration Range of 1-Ethyl-3-methylimidazolium Ethylsulfate and Water. *J. Phys. Chem. B* **2011**, *115*, 2067–2074.

(74) Kumar, S. K.; Douglas, J. F. Gelation in physically associating polymer solutions. *Phys. Rev. Lett.* **2001**, *87*, 188301.

(75) Winter, H. H.; Chambon, F. Analysis of linear viscoelasticity of a crosslinking polymer at the gel point. *J. Rheol.* **1986**, *30*, 367–382.

(76) Schwittay, C.; Mours, M.; Henningá Winter, H. Rheological expression of physical gelation in polymers. *Faraday Discuss.* **1995**, *101*, 93–104.

(77) Winter, H. H. *Structure and Dynamics of Polymer and Colloidal Systems*; Springer, 2002; pp 439–470.

(78) Fredlake, C. P.; Crosthwaite, J. M.; Hert, D. G.; Aki, S. N.; Brennecke, J. F. Thermophysical properties of imidazolium-based ionic liquids. *J. Chem. Eng. Data* **2004**, *49*, 954–964.

(79) Leys, J.; Wübbenhorst, M.; Preethy Menon, C.; Rajesh, R.; Thoen, J.; Glorieux, C.; Nockemann, P.; Thijs, B.; Binnemans, K.; Longuemart, S. Temperature dependence of the electrical conductivity of imidazolium ionic liquids. *J. Chem. Phys.* **2008**, *128*, 064509.

(80) Gibbs, J. H.; DiMarzio, E. A. Nature of the glass transition and the glassy state. *J. Chem. Phys.* **1958**, *28*, 373–383.

(81) Adam, G.; Gibbs, J. H. On the temperature dependence of cooperative relaxation properties in glass-forming liquids. *J. Chem. Phys.* **1965**, *43*, 139–146.

(82) Angell, C. A. Thermodynamic aspects of the glass transition in liquids and plastic crystals. *Pure Appl. Chem.* **1991**, *63*, 1387–1392.

(83) Martinez, L.-M.; Angell, C. A thermodynamic connection to the fragility of glass-forming liquids. *Nature* **2001**, *410*, 663–667.

(84) Del Gado, E.; Fierro, A.; de Arcangelis, L.; Coniglio, A. Slow dynamics in gelation phenomena: From chemical gels to colloidal glasses. *Phys. Rev. E* **2004**, *69*, 051103.

(85) Saika-Voivod, I.; Zaccarelli, E.; Sciortino, F.; Buldyrev, S. V.; Tartaglia, P. Effect of bond lifetime on the dynamics of a short-range attractive colloidal system. *Phys. Rev. E* **2004**, *70*, 041401.

(86) Coniglio, A.; De Arcangelis, L.; Del Gado, E.; Fierro, A.; Sator, N. Percolation, gelation and dynamical behaviour in colloids. *J. Phys. Condens. Matter* **2004**, *16*, S4831.

(87) De Candia, A.; Del Gado, E.; Fierro, A.; Sator, N.; Coniglio, A. Colloidal gelation, percolation and structural arrest. *Physica A: Statistical Mechanics and its Applications* **2005**, *358*, 239–248.

(88) Zaccarelli, E.; Buldyrev, S.; La Nave, E.; Moreno, A.; Saika-Voivod, I.; Sciortino, F.; Tartaglia, P. Model for reversible colloidal gelation. *Phys. Rev. Lett.* **2005**, *94*, 218301.

(89) Zaccarelli, E. Colloidal gels: equilibrium and non-equilibrium routes. *J. Phys. Condens. Matter* **2007**, *19*, 323101.

(90) Russo, J.; Tartaglia, P.; Sciortino, F. Reversible gels of patchy particles: Role of the valence. *J. Chem. Phys.* **2009**, *131*, 014504.

(91) Corezzi, S.; De Michele, C.; Zaccarelli, E.; Tartaglia, P.; Sciortino, F. Connecting irreversible to reversible aggregation: time and temperature. *J. Phys. Chem. B* **2009**, *113*, 1233–1236.

(92) Smallenburg, F.; Sciortino, F. Liquids more stable than crystals in particles with limited valence and flexible bonds. *Nat. Phys.* **2013**, *9*, 554–558.

(93) Lopes, J. N. A. C.; Pádua, A. A. H. Nanostructural Organization in Ionic Liquids. *J. Phys. Chem. B* **2006**, *110*, 3330–3335.

(94) Reber, D.; Grissa, R.; Becker, M.; Kühnel, R.-S.; Battaglia, C. Anion Selection Criteria for Water-in-Salt Electrolytes. *Adv. Energy Mater.* **2020**, 2002913.

(95) Sturlaugson, A. L.; Fruchey, K. S.; Fayer, M. D. Orientational Dynamics of Room Temperature Ionic Liquid/Water Mixtures: Water-Induced Structure. *J. Phys. Chem. B* **2012**, *116*, 1777–1787.

(96) Sturlaugson, A. L.; Arima, A. Y.; Bailey, H. E.; Fayer, M. D. Orientational Dynamics in a Lyotropic Room Temperature Ionic Liquid. *J. Phys. Chem. B* **2013**, *117*, 14775–14784.

(97) Chaban, V. V.; Voroshylova, I. V.; Kalugin, O. N.; Prezhdo, O. V. Acetonitrile boosts conductivity of imidazolium ionic liquids. *J. Phys. Chem. B* **2012**, *116*, 7719–7727.

(98) Singh, W. P.; Koch, U.; Singh, R. S. Gelation of ionic liquids by small-molecule gelators and their applications. *Soft Mater.* **2019**, 1–25.

(99) Li, M.; Wang, C.; Chen, Z.; Xu, K.; Lu, J. New Concepts in Electrolytes. *Chem. Rev.* **2020**, *120*, 6783—-6819.

(100) Di Noto, V.; Lavina, S.; Giffin, G. A.; Negro, E.; Scrosati, B. Polymer electrolytes: Present, past and future. *Electrochim. Acta* **2011**, *57*, 4–13.

(101) Lui, M. Y.; Crowhurst, L.; Hallett, J. P.; Hunt, P. A.; Niedermeyer, H.; Welton, T. Salts dissolved in salts: ionic liquid mixtures. *Chem. Sci.* **2011**, *2*, 1491–1496.

(102) Suo, L.; Borodin, O.; Sun, W.; Fan, X.; Yang, C.; Wang, F.; Gao, T.; Ma, Z.; Schroeder, M.; von Cresce, A., et al. Advanced High-Voltage Aqueous Lithium-Ion Battery Enabled by "Water-in-Bisalt" Electrolyte. *Angew. Chem. Int. Ed.* **2016**, *55*, 7136–7141.

(103) Chen, L.; Zhang, J.; Li, Q.; Vatamanu, J.; Ji, X.; Pollard, T. P.; Cui, C.; Hou, S.; Chen, J.; Yang, C., et al. A 63 m Super-concentrated Aqueous Electrolyte for High Energy Li-ion Batteries. *ACS Energy Lett.* **2020**, *5*, 968—974.

(104) Jiang, L.; Liu, L.; Yue, J.; Zhang, Q.; Zhou, A.; Borodin, O.; Suo, L.; Li, H.; Chen, L.; Xu, K., et al. High-Voltage Aqueous Na-Ion Battery Enabled by Inert-Cation-Assisted Water-in-Salt Electrolyte. *ADV MATER* **2020**, *32*, 1904427.

(105) Wang, F.; Borodin, O.; Ding, M. S.; Gobet, M.; Vatamanu, J.; Fan, X.; Gao, T.; Eidson, N.; Liang, Y.; Sun, W., et al. Hybrid aqueous/non-aqueous electrolyte for safe and high-energy Li-ion batteries. *Joule* **2018**, *2*, 927–937.

(106) Zhang, H.; Qin, B.; Han, J.; Passerini, S. Aqueous/Nonaqueous Hybrid Electrolyte for Sodium-Ion Batteries. *ACS Energy Lett.* **2018**, *3*, 1769–1770.

(107) Dou, Q.; Lei, S.; Wang, D.-W.; ; Zhang, Q.; Xiao, D.; Guo, H.; Wang, A.; Yang, H.; Li, Y.; Shi, S., et al. Safe and high-rate supercapacitors based on an "acetonitrile/water in salt" hybrid electrolyte. *Energy Environ. Sci.* **2018**, *11*, 3212–3219.

(108) Dou, Q.; Lu, Y.; Su, L.; Zhang, X.; Lei, S.; Bu, X.; Liu, L.; Xiao, D.; Chen, J.; Shi, S., et al. A sodium perchlorate-based hybrid electrolyte with high salt-to-water molar ratio for safe 2.5 V carbon-based supercapacitor. *Energy Storage Mater.* **2019**, *23*, 603–609.

Graphical TOC Entry